Two Years of Observations with the Chandra X-Ray Observatory (CXO)

M. C. Weisskopf

NASA Marshall Space Flight Center
Huntsville, AL 35812 USA

Cambridge, MA 02138 USA

ABSTRACT

The first x-rays detected were detected on 1999, August 12. The instrumentation is operating as expected. Together with other space observatories we are entering a new era of discovery in high-energy astrophysics.

Keywords: Chandra, CXO, space missions, x rays, grazing-incidence optics, gratings, detectors, x-ray imaging, x-ray spectroscopy, x-ray astronomy.

1. INTRODUCTION

The Chandra X-Ray Observatory (CXO) provides unprecedented capabilities for sub-arcsecond imaging, spectrometric imaging, and for high-resolution dispersive spectroscopy over the band from 0.08-10 keV. With these capabilities a wide variety of high-energy phenomena in a broad range of astronomical objects is being observed.

Chandra is a NASA facility which provides scientific data in response to scientific proposals for its use. The CXO is the result of the efforts of many government, commercial, and academic organizations, primarily located in the United States. NASA Marshall Space Flight Center (MSFC, Huntsville, Alabama) manages the Project and provides Project Science; TRW Space and Electronics Group (Redondo Beach, California) served as prime contractor; and the Smithsonian Astrophysical Observatory (SAO, Cambridge, Massachusetts) provides technical support and is responsible for ground operations including the Chandra X-ray Center (CXC). There are five scientific instruments aboard the Observatory. These instruments are discussed in §2.3 and §2.4.

The Chandra Project began in 1977 with a joint NASA/MSFC and SAO phase-A study. The study had been initiated as a result of an unsolicited proposal to NASA in 1976 by Prof. R. Giacconi and Dr. H. Tananbaum. During the intervening years, numerous milestones were reached and technical and other challenges met. These included receiving the highest recommendation by the Astronomy Survey Committee of the National Academy of Sciences, selection of the instruments, selection of the prime contractor, demonstration of the optics, restructuring of the mission, and the launch, and activation.

Invited Paper, in *X-Ray Optics, Instruments, and Missions*, P. Gorenstein & R. Hoover, eds., *Proc. SPIE* **4496**, 2001.
M.C.W.: martin@smoker.msfc.nasa.gov; 256-544-7740.

2. CHANDRA SYSTEMS

2.1. Launch and Orbit

The CXO was launched by the Space Shuttle *Columbia* and placed, briefly,into a low-earth orbit. Next, a two-stage solid-fuel rocket booster developed by the Boeing Company Defense and Space Group (Seattle, Washington) propelled the Observatory into a highly elliptical transfer orbit. Finally an internal propulsion system placed the observatory into its operational orbit - 140-Mm apogee and 10-Mm perigee, at an 28.5^o initial inclination. The orbit, with a period of 63.5 hours, yields a high (70%) observing efficiency. Uninterrupted observations lasting more than 2 days are possible.

The design life of the mission is 5 years; however, the only expendable (gas for maneuvering) is sized to allow operation for more than 10 years and the orbit will be stable for decades. NASA plans to operate the Observatory for at least 10 years.

2.2. Spacecraft

TRW Space and Electronics Group (Redondo Beach, California) built the spacecraft which includes the subsystems necessary for achieving pointing control and aspect determination, command and communications, thermal control, electrical power, etc. (See e.g. the paper by Weisskopf et al.[1])

2.3. Electron Proton Helium Instrument (EPHIN)

EPHIN[2] consists of an array of 6 silicon detectors with anti-coincidence mounted on the spacecraft near the HRMA. Built by the Institut für Experimentelle und Angewandte Physik, University of Kiel, Germany, a forerunner was flown on the SOHO satellite. The detector is used to monitor the local charged particle environment as part of the scheme to protect the focal-plane instruments from particle radiation damage and also serves as means of studying these particles.

X-Ray Optics for Astronomy: Telescopes, Multilayers, Spectrometers, and Missions, Paul Gorenstein, Richard B. Hoover, Editors, Proceedings of SPIE Vol. 4496 (2002) © 2002 SPIE · 0277-786X/02/$15.00

2.4. X-Ray Subsystems

2.4.1. High-Resolution Mirror Assembly (HRMA)

Hughes Danbury Optical Systems (HDOS, Danbury, Connecticut) figured and polished the 4 nested Wolter 1 telescopes out of Zerodur blanks (Schott Glaswerke, Mainz, Germany). The Optical Coating Laboratory Incorporated (Santa Rosa, California) coated the optics with iridium. The Eastman Kodak Company (Rochester, New York) aligned and assembled the mirrors into the 10-m focal length HRMA. A forward contamination cover houses 16 radioactive sources, developed at MSFC, for verifying transfer of the flux scale from the ground to orbit.[3–5]

2.4.2. Objective transmission gratings

Between the HRMA and the focal plane instruments are 2 objective transmission gratings (OTGs).

Low-Energy Transmission Grating (LETG) The Space Research Institute of the Netherlands (SRON, Utrecht, Netherlands) and the Max-Planck-Institüt für extraterrestrische Physik (MPE, Garching, Germany) designed and fabricated the LETG. The 540 grating facets, mounted 3 per module, lie tangent to the Rowland toroid which includes the focal plane. The LETG is constructed using free-standing gold bars of 991-nm period, and provides high-resolution spectroscopy from 0.08 to 2 keV (15 to 0.6 nm).

High-Energy Transmission Grating (HETG) The Massachusetts Institute of Technology (MIT, Cambridge, Massachusetts) designed and fabricated the HETG. The HETG has two types of facets — the Medium-Energy Gratings (MEG), mounted behind the two outermost HRMA shells, and the High-Energy Gratings (HEG), mounted behind the two innermost shells. In addition, the HEG and MEG facets are mounted 10 degrees apart in order to more easily distinguish the spectral images. The gold grating bars are polyimide-supported with 400-nm and 200-nm periods. The MEG covers the range from 0.4 to 4 keV (3 to 0.3 nm) and the HEG from 0.8 to 8 keV (1.5 to 0.15 nm).

2.4.3. Focal-plane science instruments

Chandra's two focal-plane science instruments are the (microchannel-plate) High-Resolution Camera (HRC) and the Advanced CCD Imaging Spectrometer (ACIS). Each instrument is, in turn, comprised of two imagers: one optimized for wide-field imaging and the other for reading out the high-resolution spectra dispersed by the OTGs (HRC-S with the LETG and ACIS-S with the HETG). More details on the instruments may be found in previous papers[1,6] and references therein.

3. ON-ORBIT PERFORMANCE

3.1. Imaging performance

The angular resolution of Chandra is significantly better than any previous, current, or even currently-planned x-ray observatory. Figure 1 dramatically illustrates this by comparing the official Chandra "first light", a 2.7 ks exposure of the supernova remnant Cassiopeia-A, with a ~200 ks ROSAT image. The improvement brought by Chandra's advance in angular resolution is dramatic, and the point source at the center of the remnant, undiscovered in the ROSAT image, is readily apparent in the observation with Chandra .

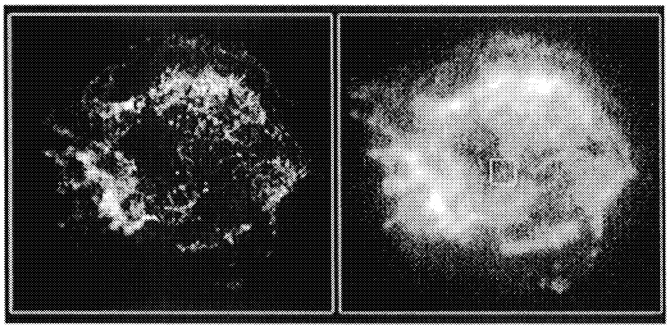

Figure 1. Chandra (left) and ROSAT (right) images of CAS-A.

Figure 2 provides a quantitative comparison of the extrapolation of the ground calibration to on-orbit performance and shows the high degree of agreement. Further details concerning the Chandra point-spread function were presented by Jerius and colleagues.[7] Additional details may be found at the relevant web sites listed at the end of this paper.

3.2. Performance anomalies

The performance of the Chandra Observatory, the instruments and subsystems have been remarkably free from problems and anomalies — a testimony to the completeness of the design and the pre-launch test program. Here we briefly discuss difficulties that have been encountered. Although these have had some impact on scientific performance, we emphasize that *no anomalies are preventing the mission from accomplishing its scientific objectives.*

3.2.1. Proton damage to the front-illuminated CCDs

After orbital activation, the energy resolution of the front-illuminated (FI) CCDs has become a function of the row number, being nearer pre-launch values close to the frame store region and progressively degraded towards the farthest row. The damage was caused by low energy protons,

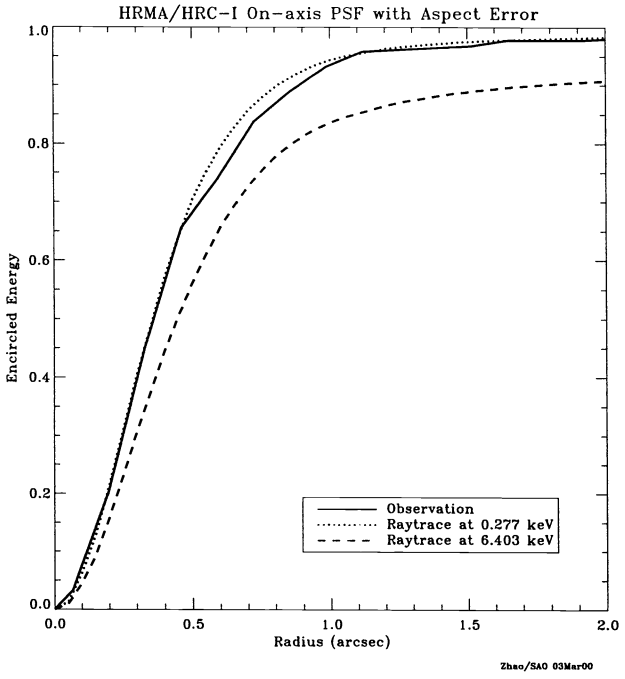

Figure 2. The predicted and observed encircled energy as a function of radius for an on-axis point source as observed with the HRC-I. The calculations, performed at two energies (0.277 and 6.40 keV) include a 0.22" contribution to simulate the impacts of uncertainties from the aspect solution. Flight data are from the calibration observation of AR Lac. Figure produced by Chandra Telescope Science.

encountered during radiation belt passages. These protons reflect off the x-ray telescope and are concentrated onto the focal plane. After altering operational procedures, the ACIS instrument is no longer left at the focal position during radiation belt passages and no further unexpected degradation in performance has been encountered. The BI CCDs were not impacted by the low-energy protons and the energy resolution for the two BI devices remains at prelaunch values. Further discussion of the proton damage may be found in various papers by members of the ACIS team.[8–10]

3.2.2. HRC anti-coincidence shield and timing

The anti-coincidence shield of the HRC-S is not working because of a timing error in the electronics. This has caused one to artificially narrow the detector in order to reduce the background counting rate below the telemetry saturation limit. In addition, the HRC was also inadvertently mis-wired so that the time of the event associated with the j-th trigger is that of the previous (j-th -1) trigger. If the data from all triggers were telemetered, the effects of the mis-wiring could be dealt with by simply reassigning the time tag, accurate to 16 μsec. New operating

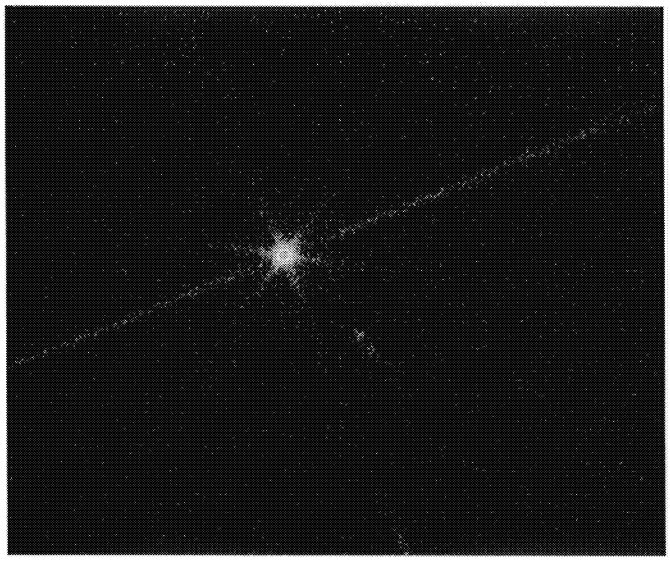

Figure 3. Image of the dispersed spectrum, including zeroth order, of 3C273. The jet is clearly resolved in the lower right hand portion of the figure. The six spikes arise from dispersion by the facet holders. Image courtesy Jeremey Drake and LETGS team.

modes have been defined which allow one to telemeter all data whenever the total counting rate is moderate to low, but at the price of higher background. For very bright sources the counting rate is so high that information associated with certain triggers are never telemetered. This situation can also be dealt with as discussed by Tennant and colleagues,[11] although with reduced time resolution.

3.3. Scientific Performance

Here we give a few examples of observations that have been performed with Chandra.

3.3.1. Imaging

Chandra's capability for high-resolution imaging enables detailed high-resolution studies of the structure of extended x-ray sources, including supernova remnants (Figure 1), astrophysical jets (Figure 3), and hot gas in galaxies and clusters of galaxies (Figure 4). The additional capability for spectrometric imaging allows studies of structure, not only in x-ray intensity, but also in temperature and chemical composition.

Furthermore, the high angular resolution permits studies of ensembles of discrete sources which would otherwise be impossible owing to source confusion. Chandra observations are able to isolate individual stars in clusters and star-forming regions and x-ray binaries in nearby normal galaxies. An example from the work of Tennant and colleagues,[13] observations of the center of M81, is shown Figure 5.

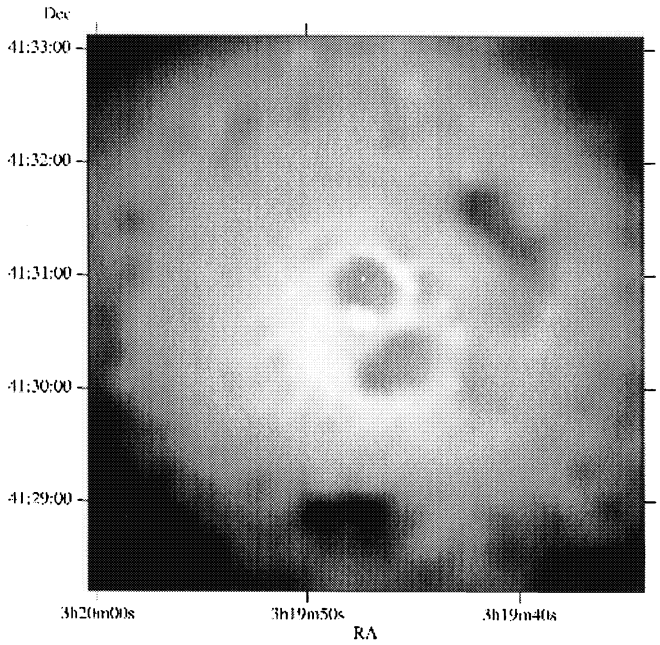

Figure 4. Adaptively smoothed 0.5-7.0 keV Chandra image of the x-ray core of the Perseus cluster from Fabian et al..[12]

High-angular-resolution observations with Chandra's low-noise focal-plane detectors are also obtaining photon-limited, deep-field exposures which are resolving most of the extragalactic cosmic x-ray background into faint, discrete sources[14,15] (Figure 6).

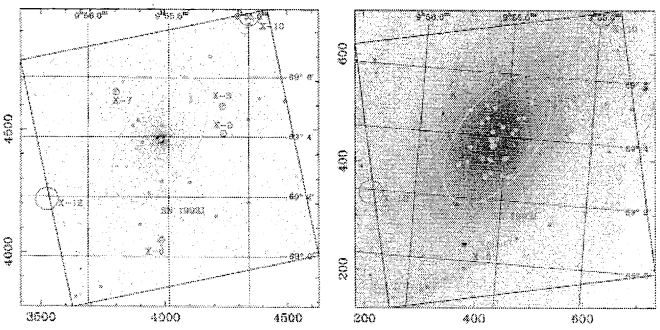

Figure 5. Chandra observations of M81. Left - x-ray image with contours. Right - x-ray contours on optical image. Image courtesy of D. Swartz.

3.3.2. Spectroscopy

Equally important are Chandra's contributions to high-resolution spectroscopy using the OTGs. These observationsare essential for determining temperature, density, elemental abundance, and ionization stage of x-ray emitting plasmas. OTG observations to date have concentrated on point sources: stellar coronae and x-ray binaries and active galactic nuclei.

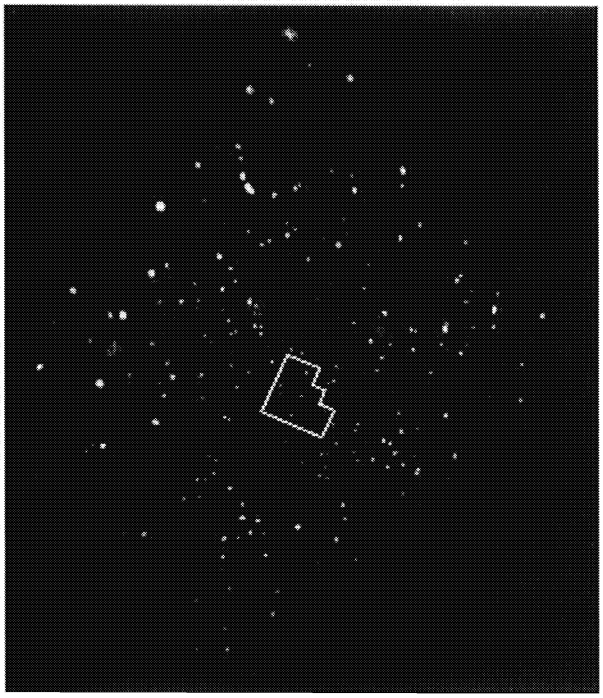

Figure 6. Chandra "true -color" ACIS image of the Chandra Deep Field - North.[14] This image has been constructed from the 0.5 -2.0 keV band (red) and 2.0 - 8.0 (blue) images. The location of the HST deep field is shown in outline. Image courtesy G. Garmire

Comparing the stellar spectra of Capella (Figure 7) and Procyon (Figure 8), one sees numerous lines but differences in the relative intensities due to the dependence on temperature. For Capella the data are from Mewe et al.[16] and for Procyon from Raassen et al..[17]

Grating spectra of the bright galactic x-ray binaries are providing new information about the material in and around the source of the x-ray emission.[18–22] One interesting example is the binary Circinus X-1,[18] thought to contain a neutron star, that at times radiates beyond its Eddington limit. The HETG spectra have lines from H-like and/or He-like Ne, Mg, Si, S and Fe. The lines exhibit broad (±2000 km/s) P Cygni profiles, with blue-shifted absorption flanking red-shifted emission (Figure 9).

High resolution spectra of AGN, especially Seyfert Galaxies, are providing new details about the physical and dynamical properties of material surrounding the

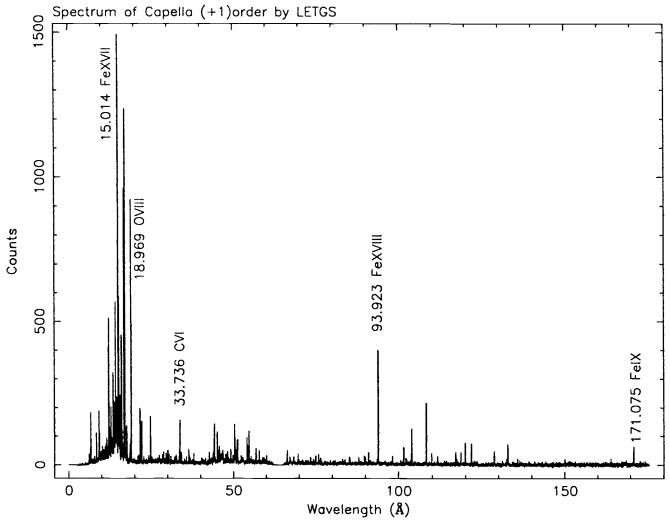

Figure 7. LETGS spectrum of Capella. Figure courtesy of B. Brinkman

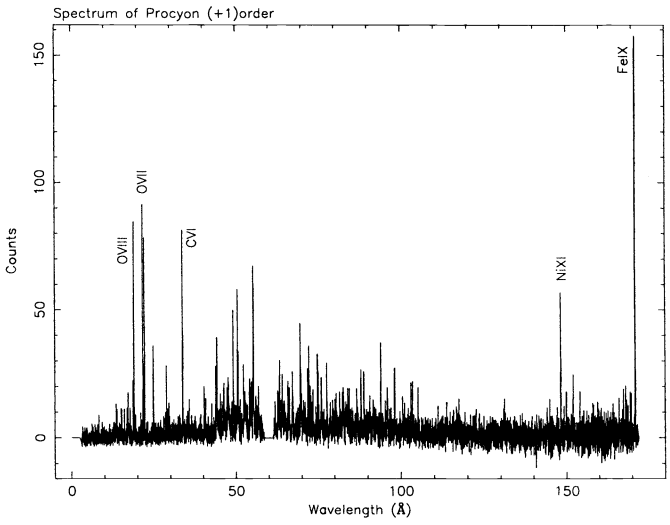

Figure 8. LETGS spectrum of Procyon. Figure courtesy of B. Brinkman

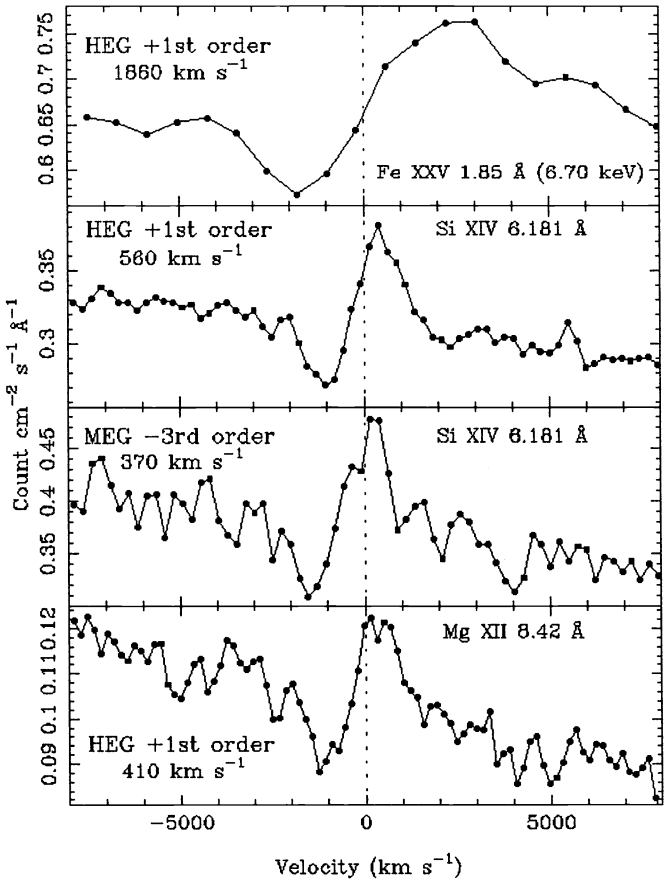

Figure 9. Several of the strongest X-ray P Cygni profiles seen from Cir X-1 with the HETG.[18]

active nucleus. For example, the LETGS spectrum of NGC 5548 shown in Figure 10 exhibits dozens of absorption lines, together with a few in emission[23] and there is evidence for bulk motions of several hundred km s^{-1}.

4. CONCLUSION

The Chandra X-Ray Observatory is performing as well, if not better, than anticipated and the results are serving to usher in a new age of astronomical and astrophysical discoveries.

5. ACKNOWLEDGEMENTS

We recognize the efforts of the many scientists and engineers that have contributed to the success of the Observatory. We especially would like to recognize the contributions of H. Tananbaum, S. O'Dell, B. Brinkman, G. Garmire, C. Canizares, S. Murray, and L.Van Speybroeck.

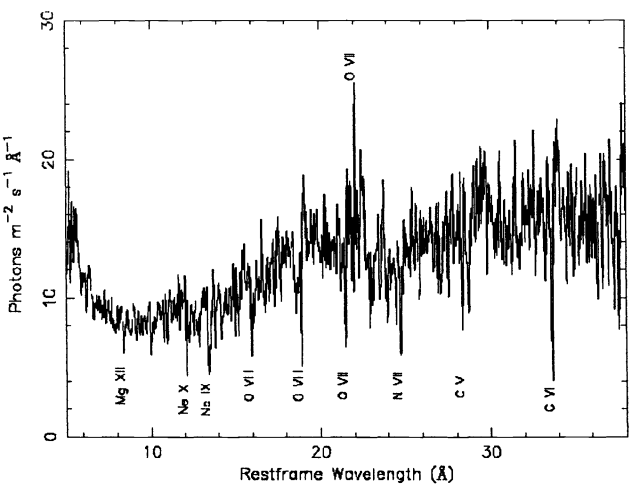

Figure 10. LETGS spectrum of the Seyfert 1 galaxy NGC 5548,[23] corrected for order contamination, redshift and Galactic absorption. Several prominent absorption lines from H-like and He-like ions are marked, as is the forbidden line of He-like oxygen.

APPENDIX A. CHANDRA WEB SITES

The following lists several Chandra-related sites on the World-Wide Web (WWW).

http://chandra.harvard.edu/ Chandra X-Ray Center (CXC), operated for NASA by the Smithsonian Astrophysical Observatory.

http://wwwastro.msfc.nasa.gov/xray/axafps.html Chandra Project Science, at the NASA Marshall Space Flight Center.

http://hea-www.harvard.edu/HRC/ Chandra High-Resolution Camera (HRC) team, at the Smithsonian Astrophysical Observatory (SAO).

http://www.astro.psu.edu/xray/axaf/axaf.html Advanced CCD Imaging Spectrometer (ACIS) team at the Pennsylvania State University (PSU).

http://acis.mit.edu/ Advanced CCD Imaging Spectrometer (ACIS) team at the Massachusetts Institute of Technology.

http://www.sron.nl/missions/Chandra Chandra Low-Energy Transmission Grating (LETG) team at the Space Research Institute of the Netherlands.

http://www.ROSAT.mpe-garching.mpg.de/axaf/ Chandra Low-Energy Transmission Grating (LETG) team at the Max-Planck Institüt für extraterrestrische Physik (MPE).

http://space.mit.edu/HETG/ Chandra High-Energy Transmission Grating (HETG) team, at the Massachusetts Institute of Technology.

http://ipa.harvard.edu/ Chandra Operations Control Center, operated for NASA by the Smithsonian Astrophysical Observatory.

http://ifkki.kernphysik.uni-kiel.de/soho EPHIN particle detector.

REFERENCES

1. M. C. Weisskopf, H. D. Tananbaum, L. P. Van Speybroeck, and S. L. O'Dell, "Chandra X-Ray Observatory: Overview," in *X-Ray Optics, Instruments, and Missions*, J. Trümper and B. Aschenbach, eds., *Proc. SPIE* **4012**, pp. 2–16, 2000.
2. R. Mueller-Mellin, H. Kunow, V. Fleissner, E. Pehlke, E.Rode, N. Roeschmann, C. Scharmberg, H. Sierks, P. Rusznyak, S. McKenna-Lawlor, I. Elendt, J. Sequeiros, D. Meziat, S. Sanchez, J. Medina, L. del Peral, M. Witte, R. Marsden, and J. Henrion, "Costep – comprehensive suprathermal and energetic particle analyser," *Solar Physics* **162**, pp. 483–504, 1995.
3. R. F. Elsner, M. K. Joy, S. L. O'Dell, B. D. Ramsey, and M. C. Weisskopf, "Ground-to-orbit transfer of the AXAF-I flux scale: In-situ contamination monitoring of x-ray telescopes," in *Multilayer and grazing incidence X-ray/EUV optics for astronomy and projection lithography*, R. B. Hoover and A. B. Walker, eds., *Proc. SPIE* **2279**, pp. 332–342, 1994.
4. R. F. Elsner, S. L. O'Dell, B. D. Ramsey, A. F. Tennant, M. C. Weisskopf, J. J. Kolodziejczak, D. A. Swartz, D. E. Engelhaupt, G. P. Garmire, J. A. Nousek, M. W. Bautz, T. J. Gaetz, and P. Zhao, "Calibration results for the AXAF flight contamination monitor," in *X-Ray Optics, Instruments, and Missions*, R. B. Hoover and A. B. Walker, eds., *Proc. SPIE* **3444**, pp. 177–188, 1998.
5. R. F. Elsner, J. J. Kolodziejczak, S. L. O'Dell, D. A. Swartz, A. F. Tennant, and M. C. Weisskopf, "Measurements with the Chandra X-Ray Observatory's flight contamination monitor," in *X-Ray Optics, Instruments, and Missions*, J. Trümper and B. Aschenbach, eds., *Proc. SPIE* **4012**, pp. 612–618, 2000.
6. M. C. Weisskopf, B. Brinkman, C. Canizares, G. Garmire, S. Murray, and L. P. Van Speybroeck, "An Overview of the Performance and Scientific Results from the Chandra X-Ray Observatory (CXO)," in *Publications of the Astronomical Society of the Pacific, PASP* **tbd**, p. tbd, 2001.

7. D. Jerius, R. H. Donnelly, M. S. Tibbetts, R. J. Edgar, T. J. Gaetz, D. A. Schwartz, L. P. Van Speybroeck, and P. Zhao, "Orbital measurement and verification of the Chandra X-ray Observatory's PSF," in *X-Ray Optics, Instruments, and Missions*, J. Trümper and B. Aschenbach, eds., *Proc. SPIE* **4012**, pp. 17–27, 2000.
8. M. W. Bautz, M. J. Pivovaroff, S. E. Kissel, G. Y. Prigozhin, T. Isobe, S. E. Jones, G. R. Ricker, R. Thornagel, S. Kraft, F. Scholze, and G. Ulm, "Absolute calibration of ACIS x-ray CCDs using undispersed synchrotron radiation," in *X-Ray Optics, Instruments, and Missions*, J. Trümper and B. Aschenbach, eds., *Proc. SPIE* **4012**, pp. 53–67, 2000.
9. G. Y. Prigozhin, S. E. Kissel, M. W. Bautz, C. Grant, B. LaMarr, R. F. Foster, G. R. Ricker, and G. P. Garmire, "Radiation damage in the Chandra x-ray CCDs," in *X-Ray Optics, Instruments, and Missions*, J. Trümper and B. Aschenbach, eds., *Proc. SPIE* **4012**, pp. 720–730, 2000.
10. G. Y. Prigozhin, M. W. Bautz, C. Grant, S. E. Kissel, B. LaMarr, and G. R. Ricker, "Characterization of the radiation damage in the Chandra x-ray CCDs," in *X-Ray and Gamma-Ray Instrumentation for Astronomy XI*, K. A. Flanagan and O. H. W. Siegmund, eds., *Proc. SPIE* **4140**, pp. –12, 2000.
11. A. F. Tennant, W. Becker, M. Juda, R. F. Elsner, J. J. Kolodziejczak, S. S. Murray, S. L. O'Dell, F. Paerels, D. A. Swartz, N. Shibazaki, and M. C. Weisskopf, "Discovery of x-ray emission from the crab pulsar at pulse minimum," *Astrophysical Journal (Letters)* **554**, pp. 173–176, 2001.
12. A. Fabian, J. Sanders, S. Ettori, G. Taylor, S. Allen, C. Crawford, K. Iwasawa, and R. Johnstone, "Chandra imaging of the x-ray core of abell 1795," *MNRAS* **319**, p. L65, 2001.
13. A. F. T. K. Wu, K. Ghosh, J. J. Kolodziejczak, and D. Swartz, "Properties of the chandra sources in m81," *Astrophysical Journal (Letters)* **549**, pp. L43–L46, 2001.
14. W. N. Brandt and et al. *Astrophysical Journal* **tbd**, pp. tbd–tbd, 2001.
15. R. Giacconi, P. Rosati, P. Tozzi, M. Nonino, G. Hasinger, C. Norman, J. Bergeron, S. Borgani, R. Gilli, R. Gilmozzi, and W. Zheng, "First results from the x-ray and optical survey of the chandra deep field south," *Astrophysical Journal* **551**, pp. 624–634, 2001.
16. R. Mewe, A. J. J. Raassen, J. S. Kaastra, R. L. vanderMeer, and D. Porquet, "Chandra-letgs x-ray observations of capella. temperature, density and abundance diagnostics," *A&A* **368**, pp. 888–900, 2001.
17. A. Raassen, R. Mewe, M. Audard, and et. al *A&A* **in preparation**, 2001.
18. W. N. Brandt and N. Schulz, "The discovery of broad p cygni lines from circinus x-1 with the chandra high-energy transmission grating spectrometer," *Astrophysical Journal* **544**, pp. L123–L128, 2000.
19. F. Paerels, A. C. Brinkman, R. L. J. van der Meer, J. S. Kaastra, E. Kuulkers, A. J. F. den Boggende, P. Predehl, J. J. Drake, S. M. Kahn, D. W. Savin, and B. McLaughlin, "Interstellar x-ray absorption spectroscopy of oxygen, neon, and iron with the chandra letgs spectrum of x0614+091," *Astrophysical Journal* **546**, pp. 338–344, 2001.
20. J. Cottam, M. Sako, S. Kahn, F. Paerels, and D. Liedahl *Astrophysical Journal* **in press**, 2001.
21. H. L. Marshall, C. R. Canizares, and N. Schulz *Astrophysical Journal* **in press**, 2001.
22. N. Schulz, D. Chakrabarty, H. Marshall, C. R. Canizares, J. Lee, and J. Houck *Astrophysical journal* **in press**, 2001.
23. J. Kaastra, R. Mewe, L. D.A., S. Komossa, and A. Brinkman, "X-ray absorption lines in the seyfert 1 galaxy ngc 5548 discovered with chandra-letgs," *A&A* **354**, pp. L83–L86, 2000.